iScience

CellPress
OPEN ACCESS

Article

Manipulating the adhesion of electroless plated Cu film on liquid polymer crystal substrate for advanced microelectronic manufacturing

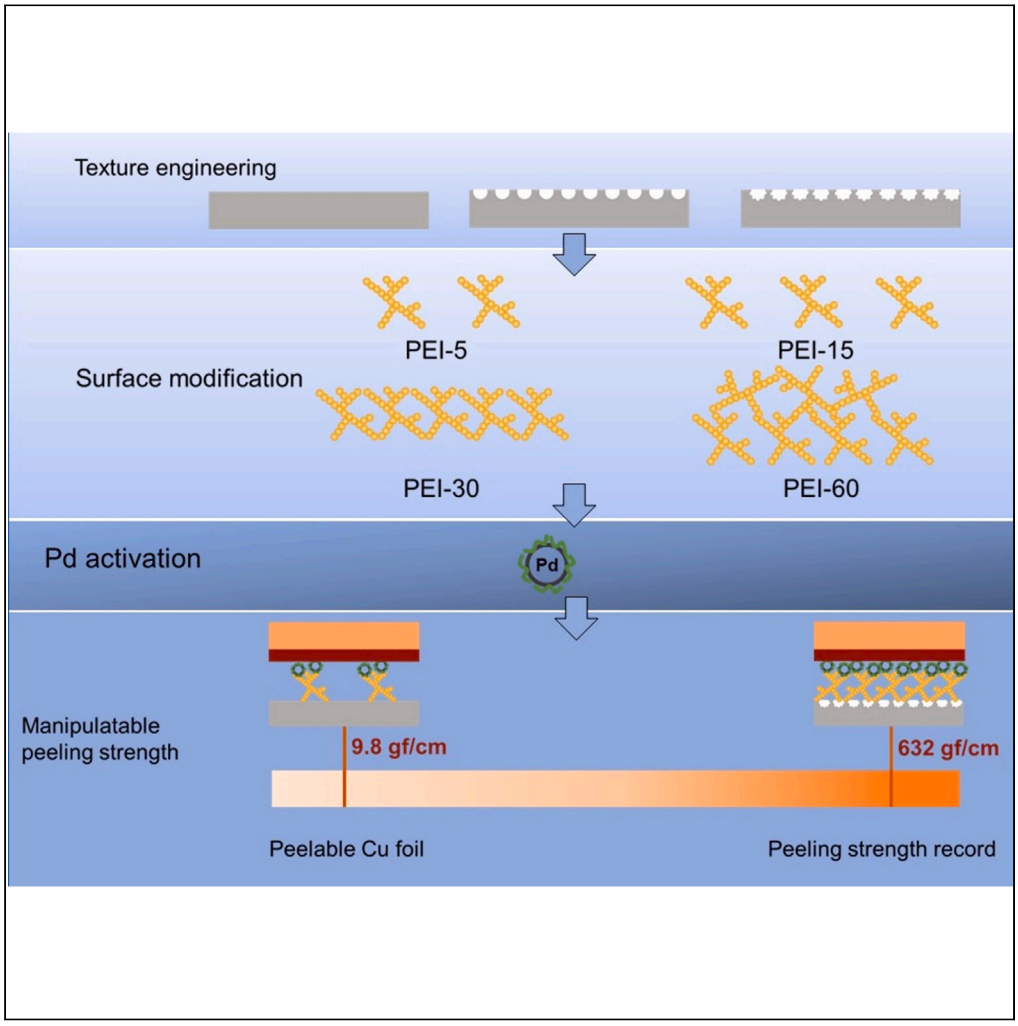

Vidya Kattoor, Pei-Tsen Wei, Zi-Fan He, Tzu-Chien Wei

tcwei@mx.nthu.edu.tw

Highlights

The peel strength of ELP Cu on LCP ranges from less than 10 gf/cm to over 600 gf/cm

Peel strength control achieved through PEI immersion time and surface roughness

Highest reported peel strength of 632 gf/cm achieved using wet-process methods on MS-CLCP

Peel strength driven by molecular interaction and physical anchoring effects

Kattoor et al., iScience 27, 111136
November 15, 2024
https://doi.org/10.1016/j.isci.2024.111136

iScience

CellPress
OPEN ACCESS

Article

Manipulating the adhesion of electroless plated Cu film on liquid polymer crystal substrate for advanced microelectronic manufacturing

Vidya Kattoor,[1] Pei-Tsen Wei,[1] Zi-Fan He,[1] and Tzu-Chien Wei[1,2,3,*]

SUMMARY

The evolution from subtractive to modified semi-additive (mSAP) and semi-additive (SAP) processes has heightened the importance of electroless plated (ELP) copper (Cu) peel strength in the printed circuit board industry. This study introduces a wet process for depositing Cu on liquid crystal polymer (LCP) using advanced electroless plating, incorporating a polyethylenimine (PEI) surfactant, a homemade nano-sized palladium (Pd) activator, and a micro-sculpturing treatment. By adjusting PEI immersion time and substrate roughness in the sub-micrometer domain, the peel strength of the ELP Cu film ranges from under 10 gf/cm to over 600 gf/cm. This wide range meets both low peel strength needs of mSAP peelable Cu foil and the high strength required in SAP. Characterization techniques, including atomic force microscopy (AFM), X-ray photoelectron spectroscopy (XPS), water contact angle (WCA) measurements, and fracture analysis, reveal that ELP Cu peel strength is driven by a synergistic effect between molecular interaction and physical anchoring.

INTRODUCTION

Printed circuit boards (PCBs) are the foundation of electronic products. They are widely used to create electronic circuits and eliminate the need for connecting wires, thereby reducing the size of a device. The manufacturing process of a PCB can be classified into two categories: subtractive method and additive method,[1] as shown in Figure 1. The subtractive method starts with the copper (Cu) clad laminate (CCL), which is a base dielectric material laminated with Cu foil (typically 20–30 μm thick). The circuitry is formed by patterning and etching away the unnecessary Cu using the photolithography procedure.[2] The subtractive method is well-established in common multilayer and high-density interconnect (HDI) PCBs. However, the subtractive method reaches its limits when the requirement for Cu width is less than 50 μm due to the irregular shape of the Cu pillar, which results from over-etching at the edge, as highlighted in Figure 1. In response to the intricate circuitry of modern electronic devices, the concept of additive manufacturing is introduced. Full additive wet process (FAP) involves selective electroless plating (ELP) of Cu on a dielectric. Although the full additive process has been scientifically proven and has triumph in creating fine Cu line, waste control, and reduces process costs, it still faces technical challenges related to the adhesion of ELP Cu and the selectivity between specific dielectric types and ELP Cu. These challenges are crucial for the manufacturability and reliability of the final PCBs. More importantly, these challenges become more critical in advanced dielectrics for high-speed, high-frequency PCB applications because modern substrates include materials like glass, liquid crystal polymer (LCP), etc., are featured with chemical inertness and low surface roughness. Semi-additive processes (SAP)[3–5] have been developed to overcome this issue. As shown in Figure 1, the SAP starts with ELP Cu on the substrate, which helps to prevent over-etching issues in the subtractive process while still ensuring manufacturability at scale. From Figure 1, it can be observed that ELP becomes increasingly important as the PCB process iterates from subtractive process to SAP. ELP is a wet process used to metallize non-conductive substrates. Compared with dry metallization methods such as sputtering or thermal evaporation, ELP is cost-effective, scalable, and has been widely utilized in PCB manufacturing.[6–8] The principle of ELP involves the catalytic reduction of metal ions from the solution onto the substrate. Palladium (Pd) is commonly used as the catalyst to lower the activation energy required for the reduction of metal ions. Generally, the adhesion of the ELP metal film to the substrate, which is an important index for the reliability of the entire circuitry, heavily depends on the surface roughness via the physical anchoring effect. Typically, the lower the roughness, the worse the adhesion becomes.

Surface roughness of the substrate can exist naturally or be formed artificially. For example, the desmear process, which is designed for removing friction-melted resin and drilling debris during through-via processing by permanganate treatment, is now widely applied to create surface roughness before ELP.[9,10] For substrates without or unable to create adequate roughness such as silicon wafer and glass, conventional ELP usually fails to provide sufficient film adhesion due to insufficient anchoring effect. Under this circumstance, chemical treatment on the

[1]Department of Chemical Engineering, National Tsing Hua University, Hsinchu City 30013, Taiwan
[2]Center for Emergent Functional Matter Science, National Yang Ming Chiao Tung University, Hsinchu, Taiwan
[3]Lead contact
*Correspondence: tcwei@mx.nthu.edu.tw
https://doi.org/10.1016/j.isci.2024.111136

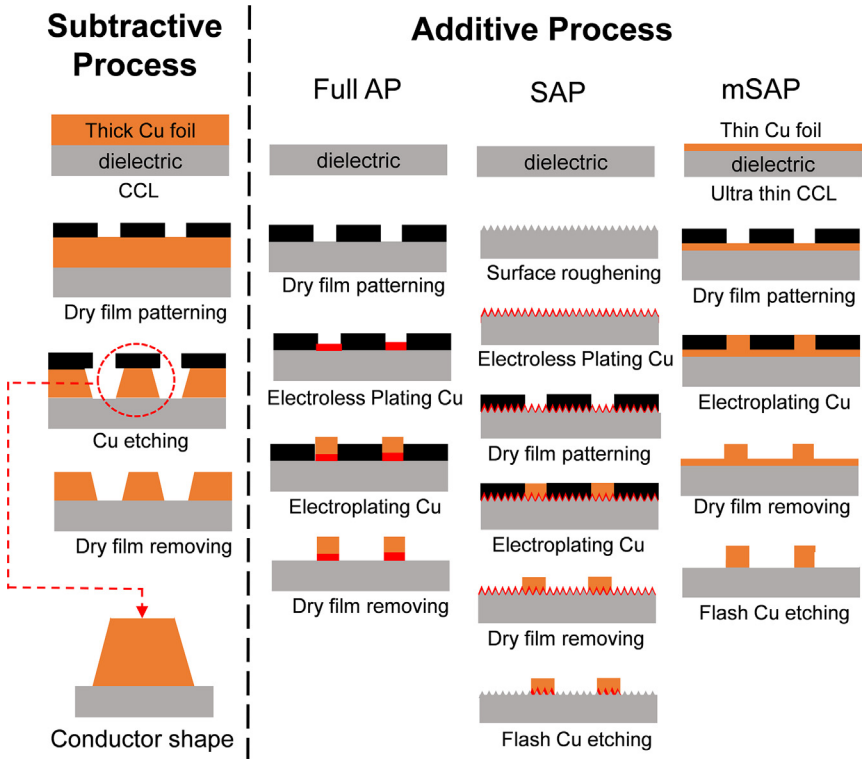

Figure 1. Diagrammatic representation of PCB manufacturing process

substrate using either silane coupling agents or surfactants is developed to enhance the adhesion of ELP film. This chemically reinforced interface can improve the adhesion of ELP film through molecular interactions such as donor-acceptor[11–13] or electrostatic effect.[14–17]

Generally, the requirement of ELP film adhesion for PCB applications is typically greater than 500 gf/cm. In the past, adequate adhesion of ELP film is obtained mechanically[18] or chemically or a combination of both methods[19–24] so that the catalysts and the subsequent metal film can be firmly anchored. However, for advanced PCBs with line widths smaller than 50 μm, such as substrate-like PCBs (SLPs) and coreless PCBs (multilayer PCBs without a core substrate), as well as for next-generation PCB dielectrics like glass and liquid crystal polymers, obtaining sufficient ELP film adhesion (500 gf/cm) remains a significant challenge. To achieve highly adhesive ELP film on these advanced substrates, several studies have explored the use of surface modification techniques,[9,19,20] the addition of adhesion-promoting layers,[11,12,16] or the application of improved Pd catalysts[13,17] to enhance the adhesion of ELP film on these substrates. However, a comprehensive solution to this challenge has yet to be fully realized.

To satisfy the demands of SLPs and coreless PCBs, a modified version of the semi-additive process (mSAP) is introduced. mSAP begins with an ultra-thin (3–5 μm) CCL to address the issue of ELP adhesion while retaining the other benefits of SAP. The ultra-thin CCL is typically made using a peelable Cu foil technology, which consists of an ultra-thin Cu foil, a releasing layer, and a carrier sandwich. After laminating the peelable Cu foil onto the dielectric, the carrier is peeled off from the sandwich to form the ultra-thin CCL. To facilitate the release of the carrier after lamination, the ultra-thin Cu foil must be weakly attached to the carrier, with a peeling strength of only 30–50 gf/cm.[25,26] This requirement is significantly different from the 500 gf/cm requirement for ELP adhesion in SAP, as mentioned earlier.

Consequently, for directly ELP onto the target substrate in SAP, a peeling strength greater than 500 gf/cm is required. In contrast, for the peelable Cu foil process, a peeling strength of less than 50 gf/cm is required. The industrial processes for these two distinct applications differ significantly due to these drastically different adhesion requirements.

In this study, we developed a single ELP process capable of meeting both high and low ELP Cu film adhesion requirements on a LCP substrate by engineering the surface modification conditions and using a novel Pd activator. LCP was chosen as the substrate due to its thermal stability, chemical inertness, low dielectric constant and loss factor up to 45 GHz, and negligible moisture effects, making it a promising next-generation PCB dielectric.[8] More importantly, achieving high adhesion for ELP directly onto LCP is challenging so it is a good candidate to investigate our novel process.[27–29] To improve adhesion between the smooth LCP surface and metal layers, we utilize the polyethylenimine (PEI), an amine-abundant surfactant,[30–32] to graft onto chemically inert LCP surface. Combined with a homemade polyvinyl alcohol-capped Pd nanoclusters (PVA-Pd) catalyst and a micro-sculpturing treatment, the peeling strength of the ELP Cu film on LCP can be manipulated over a wide range, from 9.8 to 632 gf/cm. This demonstrates the process's applicability for both high and low peeling strength requirements and paves the way for future full FAP on LCP for advanced PCBs. This study presents a process that combines surface modification, micro-sculpturing treatment, and Pd nanocluster catalysts to address the current issue of insufficient adhesion in ELP layers encountered in SAP.

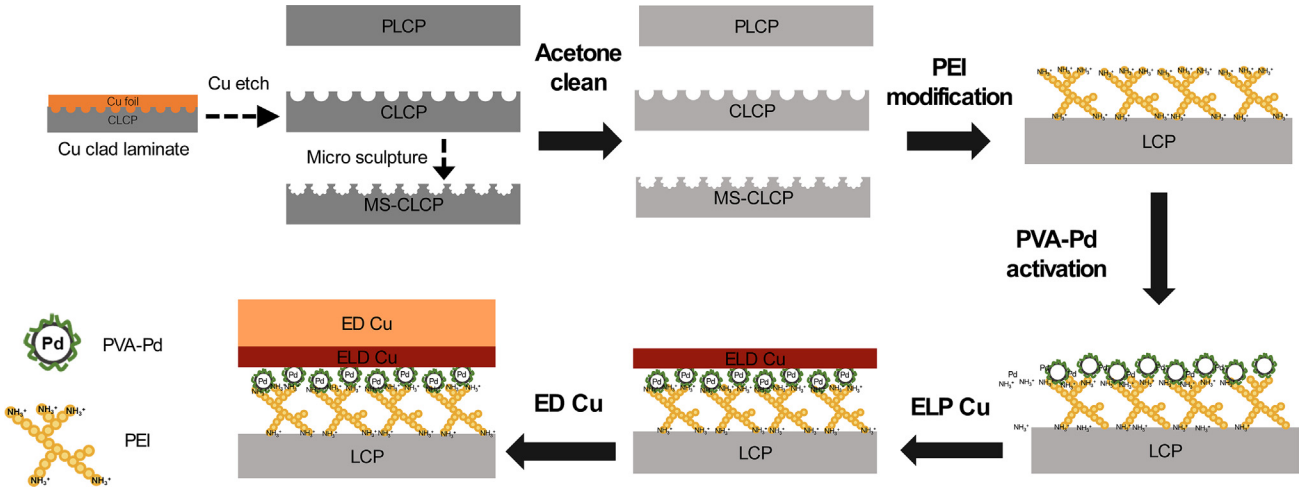

Figure 2. Schematic representation of the experimental procedure

Furthermore, our findings clarify the respective contributions of intermolecular interactions and mechanical anchoring to the adhesion of the ELP layer, providing a solid scientific foundation for the future development of advanced dielectric materials in SAP processes.

RESULTS AND DISCUSSION

In order to investigate the key causes of ELP Cu peeling strength on LCP, three types of LCP substrates (Chang Chun Plastics Co., Ltd) are investigated in this study: a pristine LCP (PLCP), an LCP substrate obtained by etching the Cu film from an LCP Cu-clad laminate (CLCP), and a micro-sculptured CLCP (MS-CLCP). PLCP has least surface roughness and is used as the substrate to study the effect of PEI modification. The surface of the CLCP has the reverse topography of the Cu layer from the original LCP CCL. The MS-CLCP is made by treating the CLCP in a modified permanganate bath containing a mixture of $KMnO_4$ (99.3%, Showa, Japan) and NaOH (50%, Showa, Japan) at 75°C for 3 min, followed by immersion in a neutralizer solution (D-830, Hurricane, Taiwan) and sulfuric acid (H_2SO_4, 98%, Union, Taiwan) at 40°C for 5 min. According to our previous study, the micro-sculpturing treatment can locally carve the surface without changing the integrity of the original landform.[31] CLCP and MS-CLCP are used to investigate the effect of surface roughness on ELP Cu peeling strength. For the ELP process, the samples are cleaned in acetone to remove organic traces and dust. After cleaning, all investigated LCP samples are treated in an aqueous PEI solution (1 v%, branched PEI, Polyscience, USA) to functionalize the surface. Before ELP in a commercial bath (THRU-CUP PEA-6, Uyemura, Japan), the PEI-modified samples are activated by PVA-Pd catalysts (50 ppm, homemade) for 5 min at room temperature. The synthesis of PVA-Pd can be found in our previous studies.[13,32] ELP Cu is carried out at 36°C for 15 min, resulting in an ELP Cu film thickness of approximately 500 nm. This is followed by thickening the ELP Cu film to 5 μm in a commercial electrodeposition bath (Macderlun, Taiwan) at 3 Amperes per square decimeter (ASD) for 9 min. The sample preparation described previously is illustrated in Figure 2.

Water contact angle (WCA) measurements (SEO, Phoenix-I, Korea) were used to assess the hydrophilicity of the substrate surfaces. Surface roughness and topography were investigated using atomic force microscopy (AFM, Nanosurf, C3000, Switzerland). Surface morphology was observed with a scanning electron microscope (SEM, Flex SEM 1000, Hitachi). Before SEM examination, a thin layer of gold was deposited on the samples by sputtering to make them conductive. The chemical environment of the samples was analyzed using X-ray photoelectron spectroscopy (XPS, VGS, Thermo K-Alpha, USA). Peeling strength measurements were performed using a 90° peel adhesion tester (90° angle peel fixture, Instron, USA).

Mechanism of PEI modification on LCP surface

The effect of branched PEI (Figure 3A) modification was studied on PLCP. Samples made by 0, 5, 15, 30, and 60 min of PEI modification are denoted as PEI-0, PEI-5, PEI-15, PEI-30, and PEI-60, respectively. Topographical SEM images are shown in Figures 3B–3F. PEI-0 exhibited extremely smooth surfaces as the surface roughness, *Sa*, which was determined using AFM (Figure S1 in the supporting information) is only 2.0 nm. Small net-like white particles appeared after PEI modification, which indicated the presence of PEI on the surface. These white particles appeared in the same fashion but became denser for prolonged PEI immersion until PEI-30. For PEI-60, these white particles appeared in an aggregated form on the surface. *Sa* of PEI-5, PEI-15, PEI-30, and PEI-60 are 3.2 nm, 4.2 nm, 2.1 nm, and 3.0 nm, respectively. According to our previous study on surface modification by soft matter,[33] the trend of *Sa* evolution upon PEI immersion time suggests PEI-5 and PEI-15 are islandish decorations and PEI-60 surface is covered by multiple layers of PEI. PEI-30 appears a relatively smallest *Sa* among all PEI-modified samples, which is a hint that PEI formed a monolayer on the surface. However, this hypothesis must be proved further.

WCA was used to probe the hydrophilicity of PEI-modified samples. Representative WCA results were shown in Figure 3, in which the averaged WCA measured from 3 samples were marked. PLCP surface before PEI modification has a WCA of 68.3°, reflecting the moderate

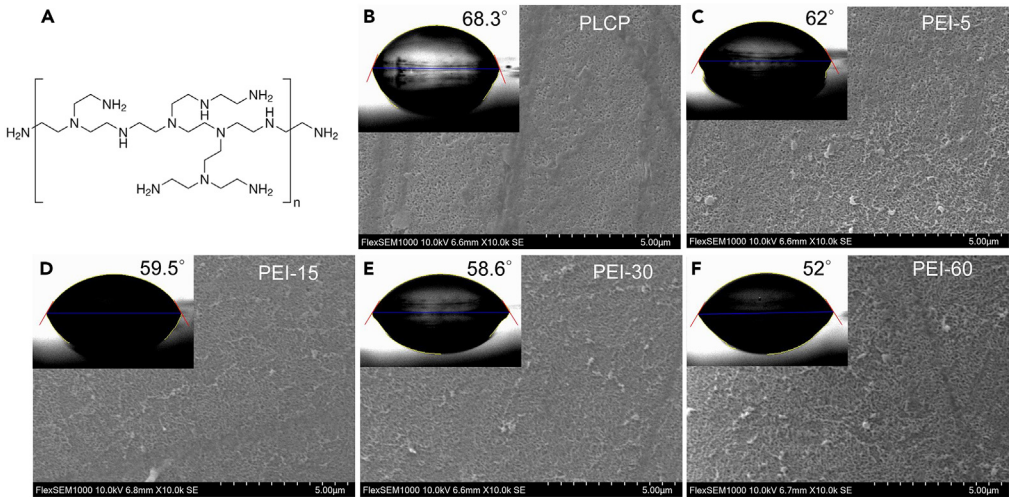

Figure 3. PEI modification on LCP surface

(A) Structure of branched PEI.

(B–F) Topographical SEM, WCA images of PLCP, and different PEI dipping time.

hydrophilicity from the aromatic polyester of LCP backbone. PEI contains abundant amine and is thus more hydrophilic than PLCP. The WCA decreased from 62.0° to 52.0° for PEI-5 to PEI-60 monotonically, evidencing PEI modification on LCP surface.

Since PEI is the only source of nitrogen atoms in the PEI-modified samples, we used the nitrogen content from XPS analysis as a quantitative indicator of PEI loading. Figure S2 shows XPS survey scans of PEI-modified samples, with the most significant change after PEI modification being the appearance of an N1s signal with a binding energy (BE) of approximately 398.0 eV. The elemental content of carbon and nitrogen from these spectra was integrated and summarized in Figure 4.

The nitrogen content increased rapidly from 0% to 5.25% for PEI-5, followed by a mild increase to 5.63% and 6.38% for PEI-15 and PEI-30, respectively. For PEI-60, there was a sharp increase to 16.13%, implying a different packing behavior of PEI from PEI-30 to PEI-60. In the initial stage of PEI immersion, the nitrogen content increased due to the attachment of PEI molecules to the open LCP substrate. As modification progresses, the LCP surface becomes increasingly occupied by PEI, hindering subsequent PEI grafting. The moderate increase in nitrogen content from PEI-5 to PEI-30 reflects this phenomenon. PEI-30 is the transition point in Figure 4 and is thus considered to form a monolayer-like PEI film. After the PEI monolayer is formed, additional PEI attaches to the existing PEI monolayer.

Since branched PEI contains abundant primary, secondary, and tertiary amine moieties, PEI attachment on the LCP surface from PEI-30 to PEI-60 becomes chaotic, forming aggregated, thick PEI layers. The dramatic increase in nitrogen content and decrease in carbon content in PEI-60 can be explained by the formation of multilayered PEI stacking, as XPS is a surface-sensitive characterization technique.

The interaction between PEI and LCP was explained using elemental XPS shown in Figure 5, where the hollow circles represent the experimental data and the red lines represent the curve-fitted results. The spectra were fitted with a Gaussian-Lorentzian function after background subtraction by the linear method. For all samples, the deconvolution of the C1s XPS spectra (Figure 5A) revealed the presence of three distinct peaks: C–C/C–H, C–O/C–N, and C=O/O–C–O. Calibration for the charging effect was performed for the C–C/C–H bond at 284.80 eV. Bare

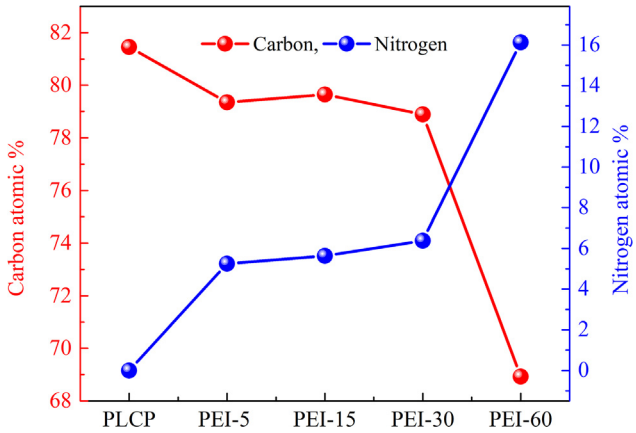

Figure 4. Carbon and nitrogen percent of LCP surface obtained in XPS with different PEI immersion time from 5 min to 60 min

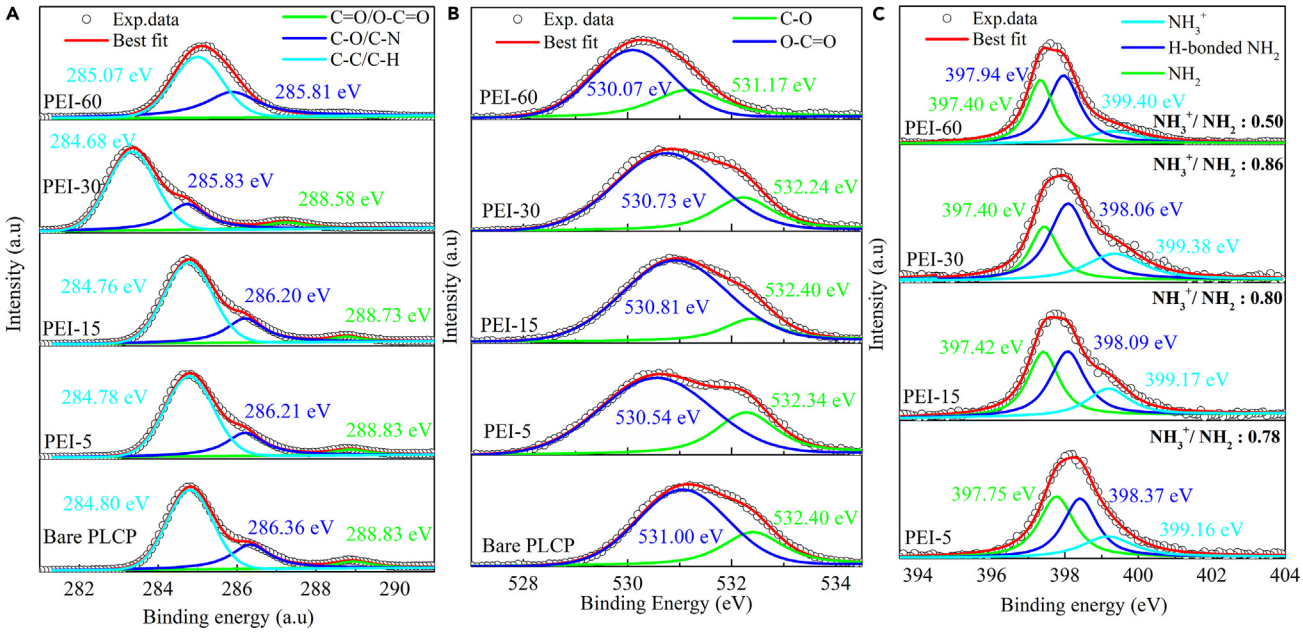

Figure 5. Study of interaction between PEI and LCP using XPS

XPS spectra of (A) C1s, (B) O1s, and (C) N 1s spectra of bare, PEI-5 min, PEI-15 min, PEI-30 min, and PEI-60 min (from bottom to top).

LCP shows C–C/C–H and C=O/O–C–O peaks at 284.80 eV and 288.83 eV, respectively, which can be treated as the constitution of the LCP backbone.

PEI modification induced a slight negative shift for both peaks up to PEI-30 (284.68 eV and 288.58 eV), indicating the interaction of PEI with the LCP surface. The peak at 286.36 eV for bare LCP also showed a negative shift after PEI modification, even though it could be from the C–O bond of the LCP backbone or from the C–N bond of the imine group (–NH) in PEI. PEI contains amino groups (–NH_2) that have an electron-donating nature. When PEI is grafted on the LCP substrate, it can chemically interact with the surface functional groups of the LCP. This interaction can change the local chemical environment around the C–C/C–H and C–O bonds, resulting in a negative shift in their XPS spectra. For PEI-60, the C–C/C–H peak showed a positive shift, while the C–O/C–N peak at 285.81 eV became broader compared to bare PLCP. Combined with the disappearance of the C=O/O–C–O peak at ~288 eV, a feature of the LCP polymer backbone, we believe the surface of PEI-60 is covered by a thick PEI layer that makes the characteristics of PLCP disappear in the XPS analysis.

The aforementioned mechanism is further supported by the O1s spectra shown in Figure 5B. The deconvoluted O1s spectra of all samples revealed two distinct peaks: C–O (532.40 eV) and O–C=O (531.00 eV). The C–O peak shows a slight negative shift up to PEI-30 (532.24 eV) and a significant negative shift to 531.17 eV for PEI-60. Similarly, the O–C=O peak shows a significant negative shift (530.07 eV) for PEI-60, indicating the same trend. Evidently, 30 min of PEI modification seems to be a point where the transition to multilayer coating of PEI on PLCP occurs. Consequently, we reasonably believe PEI-5 and PEI-15 result in island-like decoration, PEI-30 approaches monolayer coating, and PEI-60 ends with a multilayered PEI coating.

The N1s spectra (Figure 5C) of all samples show an asymmetric broad band at ~398 eV, which can be deconvoluted into three bands at 397.75, 398.37, and 399.16 eV, corresponding to free amine groups (NH_2), hydrogen-bonded amine groups (NH), and protonated amine groups (NH_{3+}), respectively. The presence of protonated and hydrogen-bonded amines arises from the interaction of PEI with itself and with the solvent (water).[34] The ratio of the deconvoluted peak intensity of NH_{3+} to NH_2 is 0.78, 0.80, 0.86, and 0.50 for PEI-5, PEI-15, PEI-30, and PEI-60, respectively, revealing a trend of increase up to 30 min of PEI immersion and then a decrease from 30 to 60 min of PEI immersion.

To understand the decrease in the ratio of NH_{3+} to NH_2, we considered the H-bonded peak intensity and calculated the ratio of hydrogen-bonded NH_2 to free NH_2, as given in Table S1. From PEI-5 to PEI-30, the ratio of H-bonded NH_2 peak intensity to free NH_2 increases (0.98–1.12) and is comparable with the ratio of NH_{3+} to NH_2 (0.78–0.86). However, in PEI-60, the ratio of H-bonded NH_2 peak intensity to free NH_2 intensity and the ratio of NH_{3+} to NH_2 became disproportionate (1.03–0.50), which strongly implies the formation of multilayered or aggregated PEI through intermolecular hydrogen bonding. As immersion time increases, the available NH_{3+} decreases, reducing the binding interaction with LCP.

Combining these results, a time-dependent mechanism for PEI modification on PLCP is proposed and schematically shown in Figure 6.

PVA-Pd uptake on PEI-modified LCP

To study the interaction of PEI with PVA-Pd, XPS analysis of PVA-Pd activated PEI-30 was conducted, and the resultant N1s and Pd3d spectra are shown in Figure 7. In Figure 7A, the BE of free amine (NH_2) and hydrogen-bonded amine shows a positive shift of 0.3 eV and 0.42 eV,

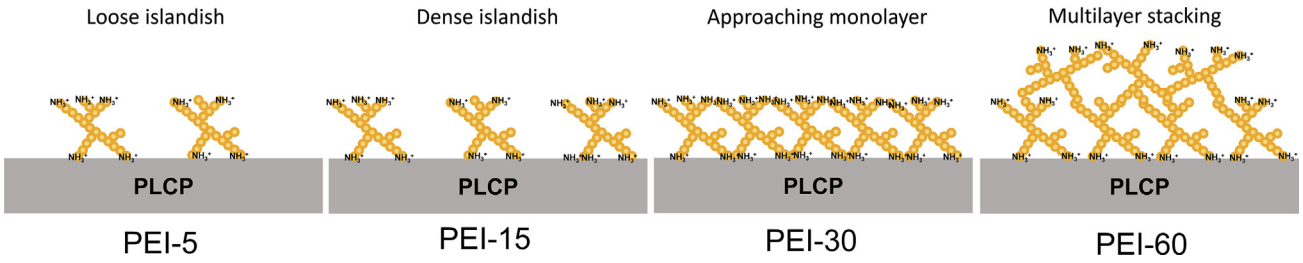

Figure 6. Schematic illustration of time-dependent PEI modification mechanism on LCP surface

respectively, after PVA-Pd uptake. Combined with the negative shift in the BE of Pd3d shown in Figure 7B, this suggests that Pd adsorption on PEI-modified PLCP follows a donor-acceptor interaction between NH_2 of PEI and the Pd core of PVA-Pd.[12,31] PVA acts as a capping agent for Pd nanoclusters and does not participate in PVA-Pd adsorption on PEI-modified LCP.

The positive shift in Figure 7A can be explained based on electronegativity. The electron-withdrawing nature of Pd causes a partial withdrawal of electron density from the neighboring amino group in the PEI polymer. This withdrawal of electron density can lead to a higher effective positive charge on the nitrogen atoms. The increased positive charge results in stronger binding of electrons to these atoms, leading to higher binding energies in the XPS spectra. In pure PVA-Pd, Pd atoms are likely in a chemical environment where they are primarily coordinated with oxygen atoms from the PVA polymer chains.[32] This coordination environment can influence the electronic properties of the Pd atoms. The presence of amino groups from PEI near the Pd atoms can influence the distribution of electron density around the Pd atoms. The electron-withdrawing nature of Pd can decrease the effective positive charge experienced by the Pd atoms. As a result, the electrons around the Pd atoms are less tightly bound, leading to a lower BE observed in Figure 7B.

Characterization of CLCP and MS-CLCP

Figure 8 summarizes the SEM and AFM topographies of PLCP, CLCP, and MS-CLCP. As mentioned previously, PLCP is very smooth with a *Sa* of merely 2.0 nm. CLCP appears sponge-like, with many craters distributed on the surface, and has a *Sa* of 130 nm. As mentioned earlier, these craters are, in fact, the reverse morphology of the Cu foil from its parental CCL. For MS-CLCP, both the top view and *Sa* (136 nm) are nearly indistinguishable from CLCP.

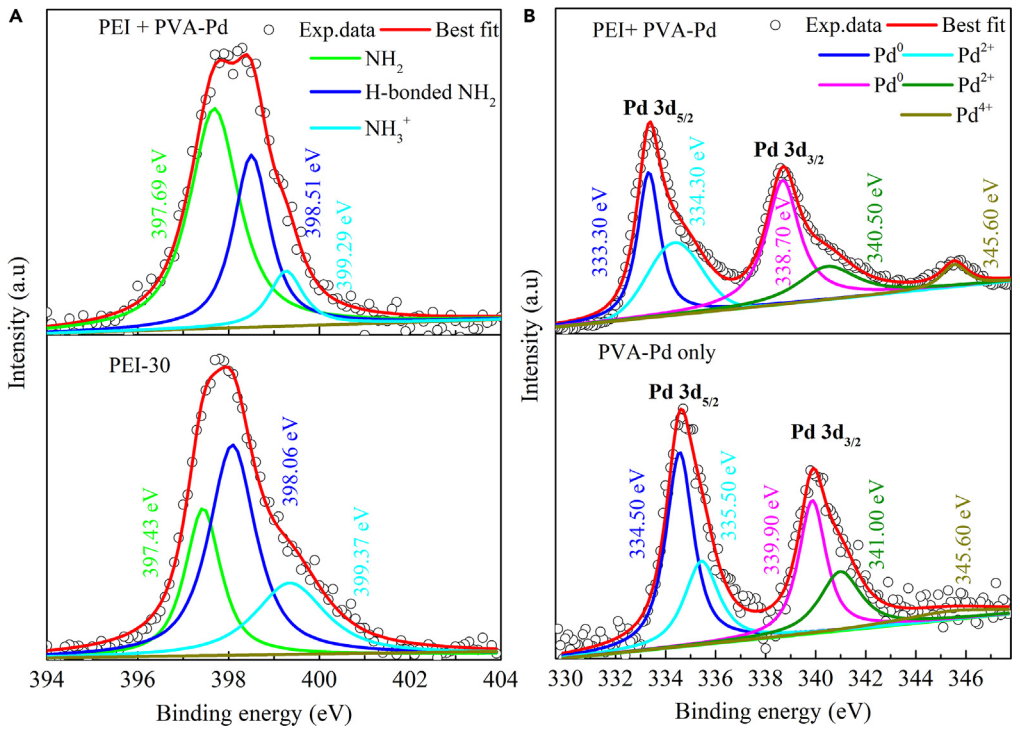

Figure 7. PVA-Pd Uptake on PEI-modified LCP

Deconvoluted XPS spectra of (A) N1s spectra of PEI-30 min (bottom) and PEI+PVA-Pd (top), (B) Pd spectra of PVA-Pd only (bottom) and PEI+PVA-Pd (top).

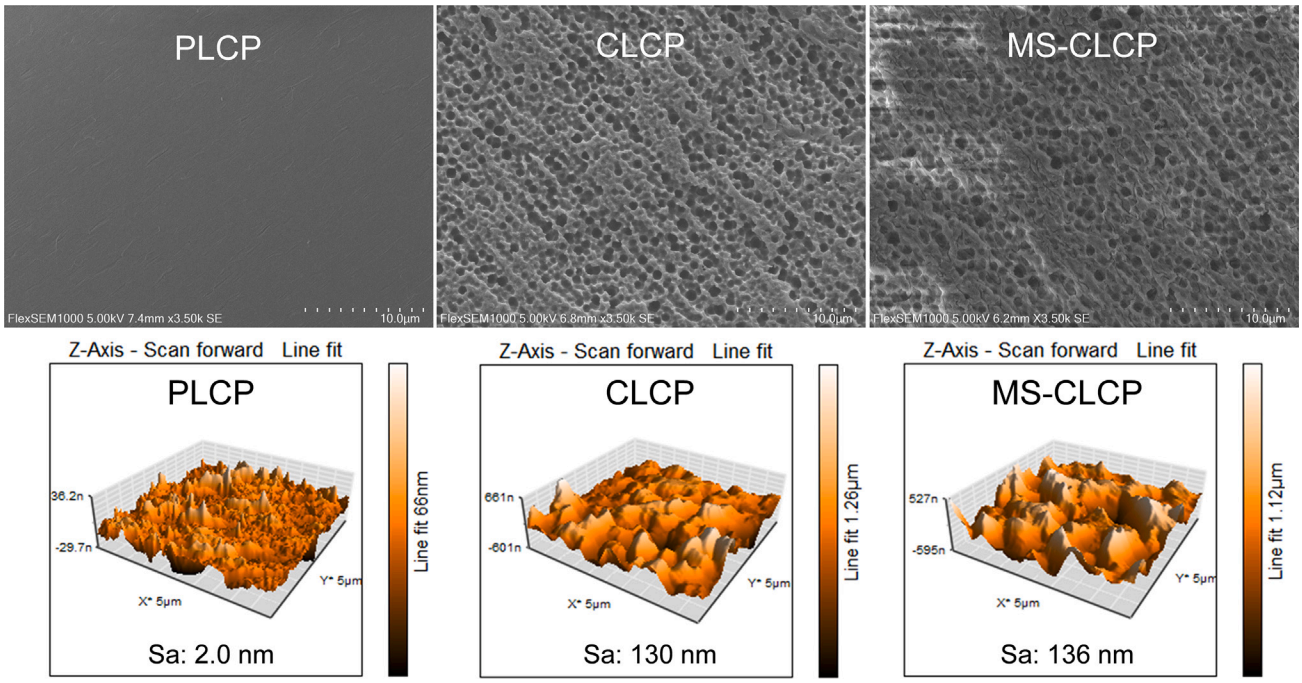

Figure 8. SEM and AFM topographic images of PLCP, CLCP, and MS-CLCP

Figure 8 summarizes SEM and AFM topographies of PLCP, CLCP, and MS-CLCP. As mentioned previously, PLCP is very smooth with *Sa* of mere 2.0 nm. CLCP appears as sponge-like as many craters distributed on the surface were seen with a *Sa* of 130 nm. These craters are in fact, the reverse morphology of the Cu foil from its parental CCL as mentioned previously. For MS-CLCP, both top view and *Sa* (136 nm) are nearly indistinguishable to CLCP.

The macroscopic surface roughness of the investigated LCP substrates was further probed using a profilometer. The average *Rq* obtained from 15 samples of PLCP, CLCP, and MS-CLCP are 5.62, 64.88, and 77.79 nm, respectively (Figure 9). It should be noted that despite CLCP and MS-CLCP being much rougher than PLCP, their surfaces are still significantly flatter than the average *Rq* (479 nm) of FR4 surfaces in traditional CCL.[31,35]

Peeling strength of ELP Cu on LCP

The peeling strength of ELP Cu on all investigated samples is shown in Figure 10. For PLCP, the adhesion of ELP Cu increases with increased PEI immersion time and peaks at PEI-30 (98 gf/cm), followed by a decrease in peeling strength for PEI-60 (51.6 gf/cm). Clearly, the adhesion of ELP Cu on PEI-modified PLCP is highly influenced by the conditions of PEI modification. As noted, the adhesion of the ELP film relies on the interaction between the amino moieties of PEI and the PVA-Pd catalyst. This explains why the ELP Cu film made with PEI-30 exhibits the highest peeling strength among all PLCP samples, as PEI-30 possesses the most abundant upright-positioned amino moieties.

ELP Cu adhesion on PEI-5 and PEI-15 is lower than on PEI-30 due to fewer amino moieties and consequently less capability to interact with PVA-Pd, resulting in poorer adhesion.[12] In PEI-60, the "effective" amino moieties are fewer than in PEI-30 due to multilayered, chaotic

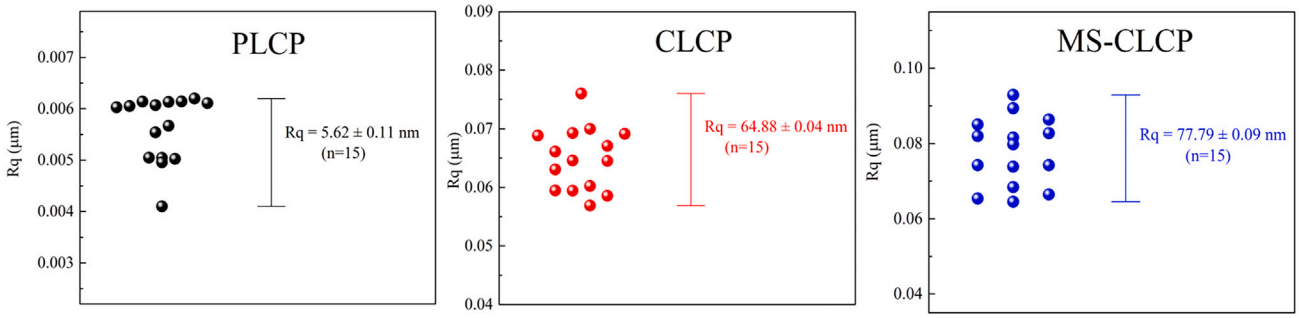

Figure 9. Rq obtained from 15 samples of PLCP, CLCP and MS-CLCP

The average Rq value of 15 samples is shown in the figure as mean ± SEM (standard error of the mean).

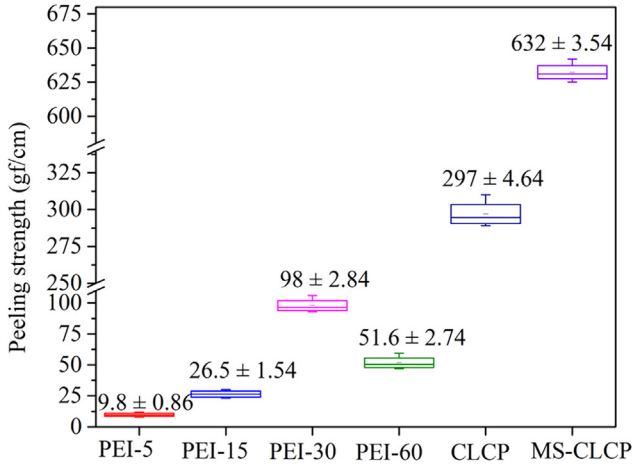

Figure 10. Averaged peeling strength of ELD Cu on investigated PEI modified PLCP, CLCP and MS-CLCP (*n* = 4)

The average peeling strength value of 4 samples (*n* = 4) shown in the figure as mean ± SEM (standard error of the mean).

stacking. XPS analysis confirms that significant amino moieties are consumed to form PEI-PEI aggregates in PEI-60. Compared to the donor-acceptor molecular interaction between PVA-Pd and PEI, the hydrogen bonding in PEI-PEI aggregates is weaker, resulting in reduced adhesion of ELP Cu despite PEI-60 having the most abundant PEI on the surface.

The peeling strengths of ELP Cu on CLCP and MS-CLCP sharply increased to 297 gf/cm and 632 gf/cm, respectively, which are approximately 3 and 6 times higher than the best peeling strength achieved on PEI-30 PLCP. This result clearly demonstrates that mechanical anchoring is more effective than molecular interaction in improving ELP Cu film adhesion, even after optimizing the molecular interaction.

SEM and energy-dispersive X-ray spectroscopy (EDS) were used for the fracture analysis of PEI-30 and PEI-60. The SEM images, elemental contributions, and schematic fracture planes are shown in Figure 11. Fracture analysis of PEI-30 (Figure 11A) indicates that all PEI remains on the LCP side, while the Cu side shows no PEI, suggesting a distinct fracture plane at the interface of PEI and PVA-Pd. For PEI-60 (Figure 11B), nitrogen signals were detected on both the LCP side and Cu side, indicating that the fracture plane lies within the PEI-PEI aggregates.

For CLCP, zoom-in SEM images of the LCP side and Cu side after the peeling test (Figure 12A) reveal that Cu was able to deposit into the craters of CLCP. The shape of the Cu deposit perfectly matches the landscape of the surface craters, indicating that our PEI treatment and PVA-Pd activator successfully provide additional physical anchoring, in addition to the molecular interaction between PEI and LCP.

In MS-CLCP (Figure 12B), the zoom-in SEM image shows that the walls of the craters became rough compared to those of its parent CLCP. The resulting Cu deposit also appears as a deflated ball-like shape instead of a spherical inflated ball, as seen in CLCP. This texture of the deflated ball-like Cu deposit was created by the micro sculpturing. The wrinkles on the Cu deposit can provide additional anchoring, which is the main reason for the high peeling strength of the ELP Cu film.

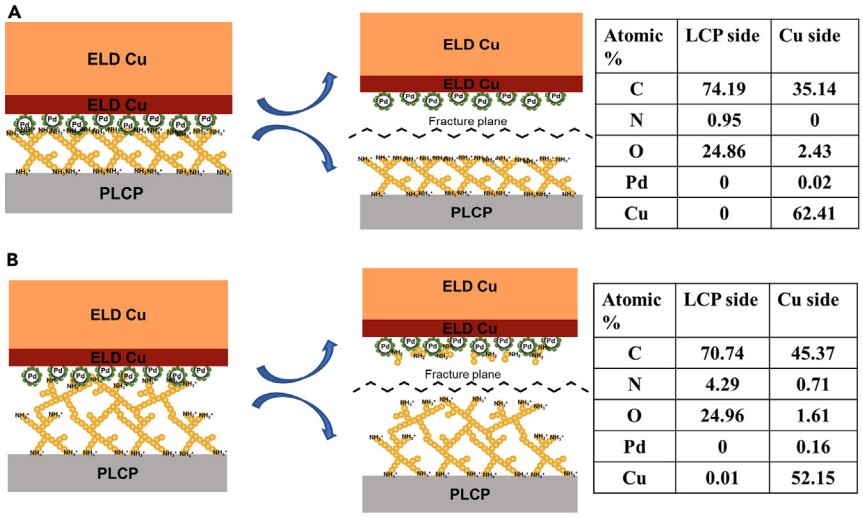

Atomic %	LCP side	Cu side
C	74.19	35.14
N	0.95	0
O	24.86	2.43
Pd	0	0.02
Cu	0	62.41

Atomic %	LCP side	Cu side
C	70.74	45.37
N	4.29	0.71
O	24.96	1.61
Pd	0	0.16
Cu	0.01	52.15

Figure 11. Imaginary fracture plane and corresponding elemental composition

Imaginary fracture plane and corresponding elemental composition of (A) PEI-30 and (B) PEI-60.

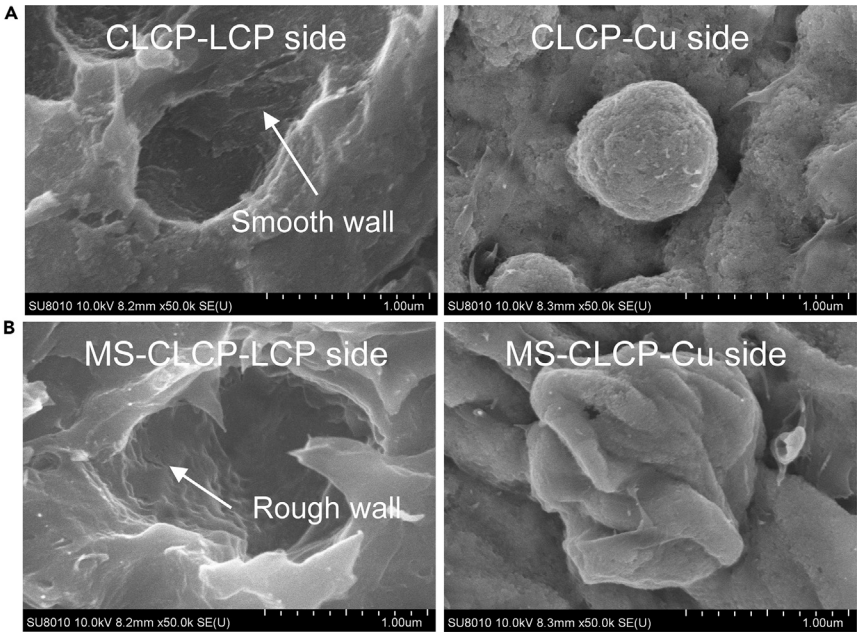

Figure 12. SEM zoom-in images of fracture analysis

SEM zoom-in images of fracture analysis of (A) CLCP and (B) MS-CLCP.

Conclusions

In conclusion, we systematically engineered the adhesion of ELP Cu on LCP substrates, aiming to understand the relationship between peeling strength and chemical, mechanical, or combined treatments. Based on our experimental findings, it is evident that establishing a molecular interaction at the interface can enhance the adhesion of ELP Cu to approximately 100 gf/cm, suitable for applications involving peelable Cu foil in mSAP processes. Furthermore, enhancing the peel strength of ELP Cu films relies significantly on the physical anchoring effects provided by surface roughness. A moderately roughened (Rq < 100 nm) cratered surface can effectively increase peel strength to approximately 300 gf/cm. By creating a hierarchical texture within these craters, peel strengths exceeding 500 gf/cm can be achieved, surpassing the requirements for ELP Cu adhesion in SAP. To our knowledge, the average peel strength of 632 gf/cm obtained on MS-CLCP represents the highest reported data for all wet-process methods.

Limitation of the study

This study focuses on the development of a highly adhesive electroless Cu plating technique on LCP substrates using PEI modification and PVA-Pd nano-Pd. The data and phenomena reported in the paper are reproducible; however, the modifiers, substrate types, and experimental conditions used in this study may not be applicable to all advanced substrates. Optimization conditions for new substrates other than LCP may need to be adjusted and refined.

RESOURCE AVAILABILITY

Lead contact

Further information and requests for resources should be directed to and will be fulfilled by the lead contact, Professor Tzu-Chien Wei (tcwei@mx.nthu.edu.tw).

Materials availability

This study did not generate new materials.

Data and code availability

- All data reported in this paper will be shared by the lead contact upon request.
- This paper does not report the original code.

ADDITIONAL RESOURCES

Our study has not generated or contributed to a new website/forum or is not part of a clinical trial.

ACKNOWLEDGMENTS

The research was funded by National Science and Technology Council, Taiwan (MOST 110-2622-8-007-015) and National Tsing Hua University, Taiwan.

AUTHOR CONTRIBUTIONS

T.-C.W. developed the idea, supervised the project and revised the manuscript; V.K. designed and carried out major experiments and drafted the manuscript. P.-T.W. and Z.-F.H. helped data collection and figure preparation. All authors reviewed the manuscript.

DECLARATION OF INTERESTS

The authors declare no competing interests.

STAR★METHODS

Detailed methods are provided in the online version of this paper and include the following:

- KEY RESOURCES TABLE
- EXPERIMENTAL MODEL AND STUDY PARTICIPANT DETAILS
- METHOD DETAILS
- QUANTIFICATION AND STATISTICAL ANALYSIS

SUPPLEMENTAL INFORMATION

Supplemental information can be found online at https://doi.org/10.1016/j.isci.2024.111136.

Received: April 29, 2024
Revised: August 20, 2024
Accepted: October 7, 2024
Published: October 10, 2024

REFERENCES

1. Chiang, Y.Y., Wang, Y.Y., and Wan, C.C. (2000). Research on applying direct plating to additive process for printed circuit board. J. Electron. Mater. *29*, 1001–1006. https://doi.org/10.1007/s11664-000-0164-7.
2. Chang, J.S., Facchetti, A.F., and Reuss, R. (2017). A circuits and systems perspective of organic/printed electronics: Review, challenges, and contemporary and emerging design approaches. IEEE J. Emerg. Sel. Top. Circuits Syst. *7*, 7–26. https://doi.org/10.1109/JETCAS.2017.2673863.
3. Iketani, S., and Vinson, M. (2020). Semi-Additive Process (SAP) Utilizing Very Uniform Ultrathin Copper by A Novel Catalyst (Santa Clara).
4. Gantz, M. (2017). mSAP: The new PCB manufacturing imperative for 5G smartphones. Electronic design. https://www.electronicdesign.com/markets/automation/article/21805746/msap-the-new-pcb-manufacturing-imperative-for-5g-smartphones.
5. Toba, M., Mitsukura, K., and Yamaguchi, M. (2021). Electroless plating with UV modification for thermosetting dielectric and decay suppression of high frequency transmission property. J. Microelectron. Electron. Packag. *18*, 51–58. https://doi.org/10.4071/imaps.1404105.
6. Cane, F.N., and Fidelity, C.P.C. (1997). Electroless plating process for the manufacture of printed circuit boards. US Patent 5648125.
7. Wang, Y., Bian, C., and Jing, X. (2013). Adhesion improvement of electroless copper plating on phenolic resin matrix composite through a tin-free sensitization process. Appl. Surf. Sci. *271*, 303–310. https://doi.org/10.1016/j.apsusc.2013.01.188.
8. Zhang, W., and Ding, D. (2016). Electroless copper plating on liquid crystal polymer films using dimethylamine borane as reducing agent. J. Chin. Chem. Soc. *63*, 222–228. https://doi.org/10.1002/jccs.201500412.
9. Park, M.S., Cho, J.C., Kim, S.H., Shin, D.J., Jung, H.m., Keun Lee, C., Cho, M.S., and Lee, Y. (2011). Optimization of desmear process for high adhesion of insulating film in printed circuit boards (PCBs) via Taguchi method. Int. J. Adhesion Adhes. *31*, 466–472. https://doi.org/10.1016/j.ijadhadh.2011.04.004.
10. Granado, L., Kempa, S., Gregoriades, L.J., Brüning, F., Bernhard, T., Flaud, V., Anglaret, E., and Fréty, N. (2019). Improvements of the epoxy–copper adhesion for microelectronic applications. ACS Appl. Electron. Mater. *1*, 1498–1505. https://doi.org/10.1021/acsaelm.9b00290.
11. Liu, T.J., Sil, M.C., and Chen, C.M. (2020). Well-organized organosilane composites for adhesion enhancement of heterojunctions. Compos. Sci. Technol. *193*, 108135. https://doi.org/10.1016/j.compscitech.2020.108135.
12. Hsu, C.W., Wang, W.Y., Wang, K.T., Chen, H.A., and Wei, T.C. (2017). Manipulating the adhesion of electroless nickel-phosphorus film on silicon wafers by silane compound modification and rapid thermal annealing. Sci. Rep. *7*, 9656. https://doi.org/10.1038/s41598-017-08639-x.
13. Hsu, C.W., Wang, W.Y., Wang, S.H., Kao, Y.H., and Wei, T.C. (2015). Adhesive Nickel-Phosphorous Electroless Plating on Silanized Silicon Wafer Catalyzed by Reactive Palladium Nanoparticles. In 10th International Microsystems, Packaging, Assembly and Circuits Technology Conference (IMPACT) (IEEE), pp. 245–249. https://doi.org/10.1109/IMPACT.2015.7365244.
14. Horiuchi, S., and Nakao, Y. (2010). Platinum colloid catalyzed etchingless gold electroless plating with strong adhesion to polymers. Surf. Coating. Technol. *204*, 3811–3817. https://doi.org/10.1016/j.surfcoat.2010.04.064.
15. Huang, Y., Pu, X., Qian, H., Chuang, C.J., Dong, S., Wu, J., Xue, J., Cheng, W., Ding, S., and Li, S. (2024). Optical fiber surface plasmon resonance sensor using electroless-plated gold film for thrombin detection. Anal. Bioanal. Chem. *416*, 1469–1483. https://doi.org/10.1007/s00216-024-05150-x.
16. Chou, S.C., Chung, W.A., Fan, T.L., Dordi, Y., Koike, J., and Wu, P.W. (2020). Polydopamine and its composite film as an adhesion layer for Cu electroless deposition on SiO2. J. Electrochem. Soc. *167*, 042507. https://doi.org/10.1149/1945-7111/ab7aa2.
17. Kohtoku, M., Honma, H., and Takai, O. (2014). Electroless Plating Catalyst Performance of a Cationic Moiety Bearing Palladium Complex. J. Electrochem. Soc. *161*, D806–D812. https://doi.org/10.1149/2.0861414jes.
18. Bamberg, S., Ralf, B., Johannes, E., and Frank, B. (2011). In IMAPSource Proceedings. Novel Wet Chemical Copper Metallization for Glass Interposers, pp. 1535–1554. https://doi.org/10.4071/2011DPC-wp12.
19. Kirmann, J., Roizard, X., Pagetti, J., and Halut, J. (1998). Effects of the alkaline permanganate etching of epoxy on the peel adhesion of electrolessly plated copper on a fibre-reinforced epoxy composite. J. Adhes. Sci. Technol. *12*, 383–397.
20. Park, M.S., Cho, J.C., Kim, S.H., Shin, D.J., Jung, H.m., Keun Lee, C., Cho, M.S., and Lee, Y. (2011). Optimization of desmear process for high adhesion of insulating film in printed circuit boards (PCBs) via Taguchi method. Int. J. Adhes. Adhes. *31*, 466–472.

21. Zhao, W., Liu, X., Song, X., Zhang, C., Chen, H., Li, X., Hui, K., Zhao, W., Qiao, L., Zhu, H., et al. (2024). Surface modification of epoxy resin by MnO_2–H_2SO_4–H_2O–$Na_4P_2O_7$ for enhanced adhesion to electroless copper. Int. J. Adhesion Adhes. *130*, 103611. https://doi.org/10.1016/j.ijadhadh.2023.103611.
22. Li, Y., Wang, Y., Wang, Y., and Wu, Y. (2023). Achieving Good Bonding Strength of the Cu Layer on PET Films by Pretreatment of a Mixed Plasma of Carbon and Copper. ACS Appl. Mater. Interfaces *15*, 12590–12602. https://doi.org/10.1021/acsami.2c23144.
23. Kataoka, T., Hirasawa, Y., Yamamoto, T., and Iwakiri, K.; Mitsui Mining and Smelting Co Ltd (2001). Making and using an ultra-thin copper foil. US Patent 6319620.
24. Takamori, M.; JX Nippon Mining and Metals Corp (2018). Method of Producing Laminated Body, and Laminated Body. US Patent 15/990970.
25. Howlader, M.M.R., Suga, T., Takahashi, A., Saijo, K., Ozawa, S., and Nanbu, K. (2005). Surface activated bonding of LCP/Cu for electronic packaging. J. Mater. Sci. *40*, 3177–3184. https://doi.org/10.1007/s10853-005-2681-5.
26. Karna, N., Joshi, G.M., and Mhaske, S.T. (2023). Structure-property relationship of silane-modified polyurethane. Prog. Org. Coat. *176*, 107377. https://doi.org/10.1016/j.porgcoat.2022.107377.
27. Aziz, T., Ullah, A., Fan, H., Jamil, M.I., Khan, F.U., Ullah, R., Iqbal, M., Ali, A., and Ullah, B. (2021). Recent progress in silane coupling agent with its emerging applications. J. Polym. Environ. *29*, 3427–3443. https://doi.org/10.1007/s10924-021-02142-1.
28. Su, W., Li, P., Yang, F., Liang, L., Huo, L., and Tang, H. (2011). Preparation and characterization of copper patterns on polyethylenimine-modified flexible substrates. React. Funct. Polym. *71*, 943–947. https://doi.org/10.1016/j.reactfunctpolym.2011.06.003.
29. Chen, J.J., An, Q., Rodriguez, R.D., Sheremet, E., Wang, Y., Sowade, E., Baumann, R.R., and Feng, Z.S. (2019). Surface modification with special morphology for the metallization of polyimide film. Appl. Surf. Sci. *487*, 503–509. https://doi.org/10.1016/j.apsusc.2019.05.016.
30. Su, W., Yao, L., Yang, F., Li, P., Chen, J., and Liang, L. (2011). Electroless plating of copper on surface-modified glass substrate. Appl. Surf. Sci. *257*, 8067–8071. https://doi.org/10.1016/j.apsusc.2011.04.100.
31. Guo, J.Y., and Wei, T.C. (2020). A Novel Wet Metallization on Photo-Imageable Dielectric Material with High T-Peel Adhesion Using Pd Nanoparticle Catalyst and Micro Surface Roughening. In 15th International Microsystems, Packaging, Assembly and Circuits Technology Conference (IMPACT) (IEEE), pp. 181–184. https://doi.org/10.1109/IMPACT50485.2020.9268588.
32. Kao, Y.H., and Wei, T.C. (2017). Novel Active Nano-Palladium Catalyst for Adhesive Electroless Plating of Ni-P Layer on Glass Interposer. In 12th International Microsystems, Packaging, Assembly and Circuits Technology Conference (IMPACT) (IEEE), pp. 130–133. https://doi.org/10.1109/IMPACT.2017.8255935.
33. Wang, W.Y., Kala, K., and Wei, T.C. (2018). Solvent-Dependent Adhesion Strength of Electroless Deposited Ni–P Layer on an Amino-Terminated Silane Compound-Modified Si Wafer. Langmuir *34*, 13597–13602. https://doi.org/10.1021/acs.langmuir.8b01927.
34. Kokufuta, E., Suzuki, H., Yoshida, R., Yamada, K., Hirata, M., and Kaneko, F. (1998). Role of hydrogen bonding and hydrophobic interaction in the volume collapse of a poly (ethylenimine) gel. Langmuir *14*, 788–795. https://doi.org/10.1021/la9709103.
35. Cai, D., and Neyer, A. (2011). Polydimethylsiloxane (PDMS) based optical interconnect with copper-clad FR4 substrates. Sensor. Actuator. B Chem. *160*, 777–783. https://doi.org/10.1016/j.snb.2011.08.062.

STAR★METHODS

KEY RESOURCES TABLE

REAGENT or RESOURCE	SOURCE	IDENTIFIER
$KMnO_4$	Showa, Japan	CAS: 7722-64-7
NaOH	Showa, Japan	CAS: 1310-73-2
Neutralizer solution (D-830)	Hurricane Co. Ltd.	D60810
Sulfuric acid (H_2SO_4, 98%)	Union chemical works Ltd.	CAS: 7664-93-9
Polyethylenimine	Polysciences, Inc.	CAS: 9002-98-6
ELP - commercial bath	Uyemura, Japan	THRU-CUP PEA-6

EXPERIMENTAL MODEL AND STUDY PARTICIPANT DETAILS

Our study does not use experimental models typical in the life sciences.

METHOD DETAILS

The synthesis of PVA-Pd can be found in our previous studies[13,32] and is briefed as follows: 285 mg of PVA (MW = 9000–10000) was dissolved in 44 mL de-ionized water at room temperature with stirring. $Pd(NO_3)_2$ (285 mg) as precursor, was added in the prepared PVA solution. 1 mL reductant (formaldehyde) was added to the prepared solution, followed by gradually adding 5 mL Na_2CO_3 (1M). The solution changed from yellowish to deep-brown immediately, indicating the formation of nano-particles, The PVA-Pd aqueous dispersion was then diluted to 50 ppm with deionized water, which is analogous to the concentration of commercial Sn/Pd colloid (C-473, OMG, USA) being used widely.

QUANTIFICATION AND STATISTICAL ANALYSIS

We report the average Rq values obtained from 15 samples of PLCP, CLCP and MS-CLCP under the same standard test conditions. The average Rq value of 4 samples are given as mean ± SEM (standard error of the mean). We also provide an average peeling strength (number of samples, $n = 4$) of ELD Cu on investigated PEI modified PLCP, CLCP and MS-CLCP. The average peeling strength value of 4 samples are given as mean ± SEM (standard error of the mean).